

# Eccentricity and elliptic flow in proton–proton collisions from parton evolution

Emil Avsar,<sup>1</sup> Christoffer Flensburg,<sup>2</sup> Yoshitaka Hatta,<sup>3</sup> Jean-Yves Ollitrault,<sup>4</sup> and Takahiro Ueda<sup>3</sup>

<sup>1</sup> 104 Davey Lab, Penn State University, University Park, 16802 PA, USA

<sup>2</sup> Dept. of Theoretical Physics, Sölvegatan 14 A, S223 62 Lund, Sweden

<sup>3</sup> Graduate School of Pure and Applied Sciences,

University of Tsukuba, Tsukuba, Ibaraki 305-8571, Japan

<sup>4</sup> CNRS, URA2306, IPhT, Institut de physique théorique, CEA Saclay, F-91191 Gif-sur-Yvette, France

(Dated: September 29, 2010)

It has been argued that high–multiplicity proton–proton collisions at the LHC may exhibit collective phenomena usually studied in the context of heavy–ion collisions, such as elliptic flow. We study this issue using a Monte Carlo implementation of the dipole cascade model. The eccentricity of the transverse area defined by the spatial distribution of produced gluons is found to be close to 40%, similar to the value in semi–central nucleus–nucleus collisions. The resulting elliptic flow is predicted to be in the range 6–7%, comparable to the value in nucleus–nucleus collisions at RHIC. Experimentally, elliptic flow is inferred from the azimuthal correlation between hadrons, which receives contributions from collective flow, and from various other effects referred to as “nonflow”. We present the first prediction for the azimuthal correlation in the absence of flow, and argue that the presence of flow is signaled by an up to 50% reduction of correlations in high–multiplicity events.

## I. INTRODUCTION

Elliptic flow is one of the most important phenomena observed in ultrarelativistic nucleus–nucleus collisions [1–3]. An Au–Au collision at RHIC produces several thousands of particles. If interactions among these particles are strong enough, they expand collectively like a fluid, and elliptic flow is a probe of this collective behavior [4]. The fluid picture is a macroscopic one, which is generally valid for a large system. For a system as small as a nucleus, it is an idealization which must be amended in order to quantitatively understand experimental data [5]. The system formed in proton–proton ( $pp$ ) collisions is even smaller. Yet the possibility has been raised that elliptic flow may be seen in  $pp$  collisions at the LHC [6–13]. This is actually a quite nontrivial problem which can only be addressed with a proper understanding of the proton wavefunction at high energy from QCD, whereas most of the preceding works [6, 9–12] are based on rather primitive models of the proton. [See, however, [7, 13].] In this letter, we study this issue using a full Monte Carlo (MC) model of the collision which implements the BFKL–type evolution of structure functions, multiple collisions, the partonic shower and the subsequent hadronization. This model is briefly described in Sec. II.

An obvious obstacle to develop collective phenomena in  $pp$  collisions is the low multiplicity of hadrons in the final state. This may be overcome by triggering on high–multiplicity events. Indeed, it has already been observed in the 7 TeV run at the LHC [14, 15] that the multiplicity distribution has a broad tail reaching out to  $\frac{dN_{ch}}{d\eta} > 30$ , and this will be further pronounced in future runs at 14 TeV. Such high–multiplicity events originate from rare fluctuations in the stochastic parton evolution of the proton and the subsequent multiple parton–parton scatterings. The fluctuations in the distribution of partons in the transverse plane then generates nonzero eccentricity

of the interaction region even in collisions at vanishing impact parameter (see Fig. 1). Assuming hydrodynamic evolution for these high–multiplicity events, we estimate the magnitude of the resulting elliptic flow in Sec. III. Our mechanism to generate an eccentricity is similar to the “hot spot” picture of [12]. Actually, the BFKL evolution considered here is *the* theory of hot spots in QCD, and is automatically included in our MC simulations.

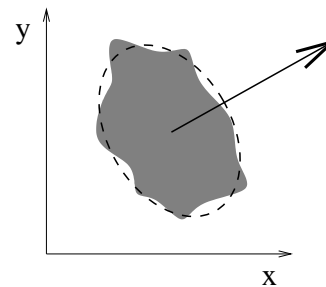


FIG. 1: Schematic picture of the initial distribution of matter in the transverse plane. The arrow indicates the direction of elliptic flow. Elliptic flow is driven by the eccentricity of the best–fitting ellipse (dashed line), denoted by  $\epsilon_{\text{part}}$ .

Experimentally, elliptic flow is not measured directly, but inferred from azimuthal correlations between the produced particles. These correlations are partly due to elliptic flow, partly due to other effects referred to as “nonflow” [16]. Nonflow correlations are sizable for peripheral nucleus–nucleus collisions at RHIC [17], and one expects them to be even larger in  $pp$  collisions, making it a challenging task to disentangle the flow contribution. In Sec. IV, we present a prediction for the azimuthal correlations using the full MC without any flow effects in the final state. By comparing the results for the correlation with or without flow, we suggest a strategy to detect flow in  $pp$  collisions at the LHC.

## II. THE MODEL

Our calculations are based on the MC implementation of the dipole model developed in Lund [18–23]. The dipole model by Mueller [24, 25] realizes the leading-order BFKL evolution of gluons (dipoles) in transverse coordinate space which is ideally suited for the computation of the eccentricity. It is known that the BFKL evolution generates large event-by-event fluctuations in the gluon multiplicity [26] as well as characteristic spatial correlations in the transverse plane [27, 28]. Both of these effects are important in properly estimating the eccentricity.

For phenomenology, the original leading-order formulation is impractical, and over the years there have been many improvements of the model which we briefly describe here. [For details, see [18–21].]

(1) Effects beyond the leading-log approximation are included via the running of the coupling and by treating energy-momentum conservation at each splitting. Energy conservation has a very large effect on the evolution and is crucial for any realistic description of the collision process.

(2) In the original formulation in [24, 25], non-linear effects are included only via the multiple interactions of dipoles from different cascades. Consequently, the scattering amplitude is no longer Lorentz invariant. Though an exact analytic treatment is missing, it has been shown that invariance can be restored to a good numerical accuracy by including the so-called “dipole swing” which mimics saturation effects in the parton evolution [19–21].

(3) The dipole splitting and interaction probabilities calculated from perturbative QCD are accurate only at short distances. In order to suppress unphysical long-distance interactions of dipoles, a finite gluon mass is introduced. This leads to propagators falling off as modified Bessel functions instead of the power-like tails obtained from the perturbative calculation. The gluon mass and the other model parameters are determined so that they reproduce the total cross section. Predictions can then be made for various other observables at different energies without any further tuning of the parameters.

The MC code that we actually use in the following, called DIPSY [22, 23], is the most advanced version by the Lund dipole team which, along with the above features, has access to all the exclusive final states. In this framework, a typical high-multiplicity event looks as follows: Before the scattering each proton develops a cascade (or ladders) of gluons spread in rapidity and the transverse plane. These gluons, mostly soft ones, then undergo multiple scatterings. The evaluation of the non-diffractive scattering amplitude for the two cascades reduces to that for individual pairs of dipoles, allowing DIPSY to decide on an event-by-event basis which dipoles interact. It is then possible to trace the interacting parton chains back from the interactions, and the initial state radiation can be identified. All emissions not connected to the interacting chains are reabsorbed as vir-

tual fluctuations. The parton chains are then passed to ARIADNE [31] that further splits the dipoles with time-like emissions. After that the dipoles hadronize through the string fragmentation model in PYTHIA [32, 33], giving final states.

## III. ELLIPTIC FLOW FROM THE ECCENTRICITY

In a nucleus-nucleus collision, the participant eccentricity  $\epsilon_{\text{part}}$  (see Fig. 1) is defined from the positions  $(x, y)$  of participant nucleons within the nucleus [3]:

$$\epsilon_{\text{part}} \equiv \frac{\sqrt{(\sigma_y^2 - \sigma_x^2)^2 + 4\sigma_{xy}^2}}{\sigma_y^2 + \sigma_x^2}, \quad (1)$$

where

$$\begin{aligned} \sigma_x^2 &= \{x^2\} - \{x\}^2, \\ \sigma_y^2 &= \{y^2\} - \{y\}^2, \\ \sigma_{xy} &= \{xy\} - \{x\}\{y\}, \end{aligned} \quad (2)$$

and the brackets  $\{\dots\}$  denote averaging over the participants in a given event. We shall be interested in the quantities  $\epsilon\{2\}$  and  $\epsilon\{4\}$  defined by

$$\epsilon\{2\} \equiv \sqrt{\langle \epsilon_{\text{part}}^2 \rangle}, \quad (3)$$

and

$$\epsilon\{4\} \equiv (2\langle \epsilon_{\text{part}}^2 \rangle^2 - \langle \epsilon_{\text{part}}^4 \rangle)^{1/4}, \quad (4)$$

where  $\langle \dots \rangle$  denotes averaging over events in a given centrality bin. Hydrodynamic evolution linearly relates  $\epsilon\{n\}$  and the corresponding elliptic flow  $v_2\{n\}$  measured from the  $n$ -particle azimuthal correlation [29]. An empirical formula which works at RHIC is [5]

$$v_2\{2\} = \epsilon\{2\} \left( \frac{v_2}{\epsilon} \right)^{\text{hydro}} \frac{1}{1 + \frac{\bar{\lambda}}{K_0} \frac{\langle S \rangle}{\frac{dN}{d\eta}}}, \quad (5)$$

and a similar relation between  $v_2\{4\}$  and  $\epsilon\{4\}$ . In (5),  $(v_2/\epsilon)^{\text{hydro}} \approx 0.2$  is the ideal hydrodynamics result and the parameter  $\bar{\lambda}/K_0 = 5.8 \text{ fm}^{-2}$  measures the degree of incomplete equilibration.  $S$  is the area of the overlap region calculated as

$$S = 4\pi \sqrt{\sigma_x^2 \sigma_y^2 - \sigma_{xy}^2}, \quad (6)$$

and  $\frac{dN}{d\eta} \approx 1.5 \frac{dN_{ch}}{d\eta}$  is the total hadron rapidity distribution. [We neglect the small difference between the rapidity and the pseudorapidity.]

In  $pp$  collisions, we employ the same formulae (1)–(4) but this time the averaging in (2) is performed for the “liberated” gluons, i.e., those in the initial state radiation.

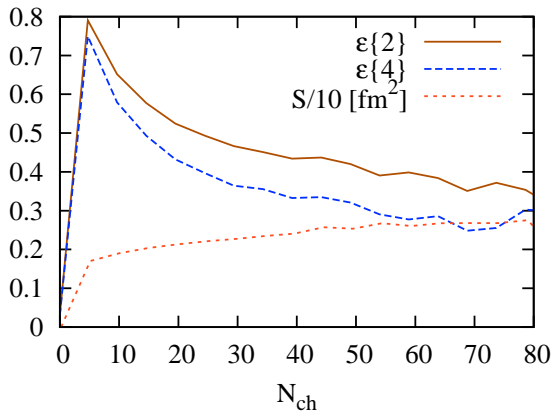


FIG. 2: (Color online) Predictions for the eccentricity and the interaction area at 7 TeV.

As the collective motion is associated with centrally produced particles, we apply a rapidity cut such that only gluons which are separated from the beam directions by more than 2 units of rapidity are included in the averaging (2).

We have generated  $pp$  events at  $\sqrt{s}=7$  TeV and 14 TeV with randomly chosen impact parameter  $\vec{b}$ , and classified events in bins of the charged particle multiplicity  $N_{ch}$ . The averaging  $\langle \dots \rangle$  has been taken in each bin. Unlike in nucleus–nucleus collisions, in  $pp$  collisions the impact parameter is not measurable, and there is no simple scaling between the centrality and the multiplicity because of the fluctuations. Still, we can safely say that the highest–multiplicity events predominantly arise from collisions with  $b \approx 0$ .

If the rescatterings among liberated partons (not included in DIPSY) are strong enough, nonzero  $\epsilon$  will give rise to  $v_2$  according to the formula (5). In Figs. 2 and 3, we plot the results for  $\epsilon$  and  $v_2$  (labeled “flow”), respectively, as a function of  $N_{ch}$  within the ALICE acceptance  $|\eta| < 0.9$  (central detector). For determining  $N_{ch}$  (or  $dN/d\eta$ ) in each event, we assume that it is proportional to the number of dipole–dipole subcollisions,  $N_{ch} \propto N_{col}$ , and we fix the proportionality constant using the low– $N_{ch}$  events where collective motion is not expected and hence the full MC (i.e., with final states) can be used. Events with  $N_{ch} = 60$  typically have  $N_{col}$  as large as 12 at 7 TeV.

We see that  $v_2$  is about 6–7% and is roughly independent of  $N_{ch}$ , though of course the low– $N_{ch}$  region should not be taken seriously. This is comparable to the value in Au–Au collisions at RHIC. We do not see any significant difference between 7 and 14 TeV even though high–multiplicity events are more frequent at 14 TeV.

It is worth noting that the conventional definition of the eccentricity

$$\epsilon_s \equiv \frac{\sigma_y^2 - \sigma_x^2}{\sigma_y^2 + \sigma_x^2}, \quad (7)$$

typically takes a negative value, if the impact parameter is chosen in the  $x$ –direction. This is in stark contrast to the nucleus–nucleus case where the interaction region is roughly the geometrical overlap of two colliding nuclei so that  $\epsilon_s > 0$  always. While  $\epsilon_s$  is unmeasurable in  $pp$  collisions, this still illustrates the fact that the origin of the eccentricity is very different from that in the nucleus–nucleus case.

#### IV. THE TWO–PARTICLE AZIMUTHAL CORRELATION

Experimentally in nucleus–nucleus collisions, elliptic flow is usually analyzed using the event–plane method [30]. A simpler method, which is almost equivalent [17], uses two–particle correlations between outgoing particles. The corresponding estimate of elliptic flow is defined by

$$v_2\{2\} = \sqrt{\langle \{ \cos(2(\phi_i - \phi_j)) \} \rangle}, \quad (8)$$

where  $\phi_i$  is the azimuthal angle of the  $i$ –th outgoing particle, and the averaging is over all pairs in the final state satisfying some cut requirements.

At the LHC, one expects a large  $v_2\{2\}$  even without collective flow, due to copious jet production. To estimate the correlation not associated with flow, we compute (8) from exclusive final states generated by DIPSY. The result is presented in Fig. 3 (labeled “nonflow”) as a function of  $N_{ch}$ , also obtained from DIPSY. No cut in  $p_t$  is imposed. We find that  $v_2$  is about a factor of 2 larger than the “flow” case. The value is more or less constant in  $N_{ch}$ , though we see some evidence that on event–by–event basis the final states look more rounded (as opposed to “jetty”) at larger  $N_{ch}$ . Again we do not

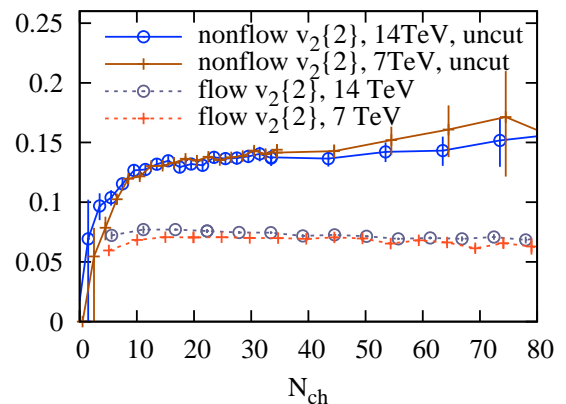


FIG. 3: (Color online) Predictions for  $v_2\{2\}$  calculated from Eq. (5) (“flow”) and Eq. (8) (“nonflow”) versus charged multiplicity at  $\sqrt{s} = 7$  TeV and 14 TeV. The error bars in the “flow” data are smaller than the points.

see any significant difference between the 7 and 14 TeV results.

## V. DISCUSSION

In the previous sections, we have calculated  $v_2$  in two different ways which are based on two extreme scenarios. In Sec. III, it is assumed that the entire system in the interaction region evolves into flow, whereas in Sec. IV there is no flow at all in the final state no matter how large  $N_{ch}$  becomes. A more realistic situation must lie somewhere in between, involving both flow and nonflow components at the same time. Thus we have actually determined the lower and upper bounds of  $v_2$ .

In the low- $N_{ch}$  region there is certainly no flow, and according to our prediction  $v_2$  stays large, at around 13–14%. The question is then what happens at large  $N_{ch}$ . From a conservative standpoint, one may presume that there is never any kind of collective behavior in  $pp$ . If this is the case,  $v_2$  should remain roughly constant. However, an exciting scenario is that the system eventually starts to develop some degree of collectivity, in which case we see that  $v_2$  will deviate downwards as  $N_{ch}$  increases. The

maximal reduction in  $v_2$  will be up to 50% in the ideal hydro limit, but in practice we expect a correction of order  $1/N_{ch}$  due to nonflow effects [30].

It should be straightforward to compute (8) using the already available experimental data at the LHC. In the low- $N_{ch}$  region this will be a test of the MC, and if reproduced, it will support the credibility of our prediction at larger  $N_{ch}$ . Data will then tell us whether we are entering a new and interesting region of hadronic collisions at high energy.

## Acknowledgements

We are grateful to Gösta Gustafson and Leif Lönnblad for allowing us to use DIPSY, prior to publication [23], for this particular observable. We thank Alejandro Alonso and the participants of the workshop “High Energy Strong Interactions 2010” at Yukawa Institute, for discussions. The work of Y. H. and T. U. is supported by Special Coordination Funds for Promoting Science and Technology of the Ministry of Education, the Japanese Government. E. A. is supported by the US D.O.E. grant number DE-FG02-90-ER-40577.

- 
- [1] K. H. Ackermann *et al.* [STAR Collaboration], Phys. Rev. Lett. **86**, 402 (2001) [arXiv:nucl-ex/0009011].
  - [2] S. S. Adler *et al.* [PHENIX Collaboration], Phys. Rev. Lett. **91**, 182301 (2003) [arXiv:nucl-ex/0305013].
  - [3] B. Alver *et al.* [PHOBOS Collaboration], Phys. Rev. Lett. **98**, 242302 (2007) [arXiv:nucl-ex/0610037].
  - [4] J. Y. Ollitrault, Phys. Rev. D **46**, 229 (1992).
  - [5] H. J. Drescher, A. Dumitru, C. Gombeaud and J. Y. Ollitrault, Phys. Rev. C **76**, 024905 (2007) [arXiv:0704.3553 [nucl-th]].
  - [6] M. Luzum and P. Romatschke, Phys. Rev. Lett. **103**, 262302 (2009) [arXiv:0901.4588 [nucl-th]].
  - [7] I. Bautista, L. Cunqueiro, J. D. de Deus and C. Pajares, J. Phys. G **37**, 015103 (2010) [arXiv:0905.3058 [hep-ph]].
  - [8] Z. Chajacki and M. Lisa, Nucl. Phys. A **830**, 199C (2009) [arXiv:0907.3870 [nucl-th]].
  - [9] S. K. Prasad, V. Roy, S. Chattopadhyay and A. K. Chaudhuri, Phys. Rev. C **82**, 024909 (2010) [arXiv:0910.4844 [nucl-th]].
  - [10] D. d’Enterria, G. K. Eyyubova, V. L. Korotkikh, I. P. Lokhtin, S. V. Petrushanko, L. I. Sarycheva and A. M. Snigirev, Eur. Phys. J. C **66**, 173 (2010) [arXiv:0910.3029 [hep-ph]].
  - [11] P. Bozek, Acta Phys. Polon. B **41**, 837 (2010) [arXiv:0911.2392 [nucl-th]].
  - [12] J. Casalderrey-Solana and U. A. Wiedemann, Phys. Rev. Lett. **104**, 102301 (2010) [arXiv:0911.4400 [hep-ph]].
  - [13] T. Pierog, S. Porteboeuf, I. Karpenko and K. Werner, arXiv:1005.4526 [hep-ph].
  - [14] K. Aamodt *et al.* [ALICE Collaboration], Eur. Phys. J. C **68**, 345 (2010) [arXiv:1004.3514 [hep-ex]].
  - [15] CMS Collaboration, arXiv:1009.4122 [hep-ex].
  - [16] P. M. Dinh, N. Borghini and J. Y. Ollitrault, Phys. Lett. B **477**, 51 (2000) [arXiv:nucl-th/9912013].
  - [17] J. Y. Ollitrault, A. M. Poskanzer and S. A. Voloshin, Phys. Rev. C **80**, 014904 (2009) [arXiv:0904.2315 [nucl-ex]].
  - [18] E. Avsar, G. Gustafson and L. Lönnblad, JHEP **0507**, 062 (2005) [arXiv:hep-ph/0503181].
  - [19] E. Avsar, G. Gustafson and L. Lönnblad, JHEP **0701**, 012 (2007) [arXiv:hep-ph/0610157].
  - [20] E. Avsar, G. Gustafson and L. Lönnblad, JHEP **0712**, 012 (2007) [arXiv:0709.1368 [hep-ph]].
  - [21] C. Flensburg, G. Gustafson and L. Lönnblad, Eur. Phys. J. C **60**, 233 (2009) [arXiv:0807.0325 [hep-ph]].
  - [22] C. Flensburg, arXiv:1009.5323 [hep-ph].
  - [23] C. Flensburg, G. Gustafson and L. Lönnblad, to appear.
  - [24] A. H. Mueller, Nucl. Phys. B **415**, 373 (1994).
  - [25] A. H. Mueller, Nucl. Phys. B **437**, 107 (1995) [arXiv:hep-ph/9408245].
  - [26] G. P. Salam, Nucl. Phys. B **449**, 589 (1995) [arXiv:hep-ph/9504284].
  - [27] Y. Hatta and A. H. Mueller, Nucl. Phys. A **789**, 285 (2007) [arXiv:hep-ph/0702023].
  - [28] E. Avsar and Y. Hatta, JHEP **0809**, 102 (2008) [arXiv:0805.0710 [hep-ph]].
  - [29] R. S. Bhalerao and J. Y. Ollitrault, Phys. Lett. B **641**, 260 (2006) [arXiv:nucl-th/0607009].
  - [30] A. M. Poskanzer and S. A. Voloshin, Phys. Rev. C **58**, 1671 (1998) [arXiv:nucl-ex/9805001].
  - [31] L. Lönnblad, Comput. Phys. Commun. **71**, 15 (1992).
  - [32] T. Sjostrand, S. Mrenna and P. Z. Skands, JHEP **0605**, 026 (2006) [arXiv:hep-ph/0603175].
  - [33] B. Andersson, G. Gustafson, G. Ingelman, and T. Sjostrand, Phys. Rept. **97**, 31 (1983).